Rapid Transcriptional Activity *in Vivo* and Slow DNA Binding *in Vitro* by an Artificial Multi-Zinc Finger Protein[†]

Tatsuya Morisaki,[‡] Miki Imanishi,*[,‡,§] Shiroh Futaki,[‡] and Yukio Sugiura*[,||]

Institute for Chemical Research, Kyoto University, Uji, Kyoto 611-0011, Japan, PRESTO, Japan Science and Technology Agency (JST), Kawaguchi, Saitama 332-0012, Japan, and Faculty of Pharmaceutical Sciences, Doshisha Women's University, Kyotanabe, Kyoto 610-0395, Japan

Received June 16, 2008; Revised Manuscript Received July 22, 2008

ABSTRACT: Artificial transcription factors targeting any desired genes are very attractive but require specific DNA binding domains in order to address a single site for each gene promoter. By connecting various zinc fingers recognizing the corresponding 3−4 bp DNA, DNA binding domains for the desired and long sequences can be created. Though such a long sequence recognition is a marvelous property, we have found that as the number of finger motifs increases, the equilibrium time with the target sequence is significantly longer as detected by *in vitro* EMSA experiments. In this study, we created 3- and 9-finger-type artificial transcription factors and compared the kinetics of the transcriptional activation *in vivo* as to whether or not a significant delay in the activation is observed for the 9-finger type. By using a ligand-inducing system, we demonstrated for the first time that finger multimerization does not affect the kinetics of the transcriptional activity; the 9-finger type artificial transcription factor activated the reporter gene as quickly as the 3-figner type. Our results suggest that the drawback of finger multimerization, i.e., the equilibrium time is prolonged depending on the number of finger motifs, can be surmounted in terms of its use for transcription factors *in vivo*. There is much interest in creating therapeutic molecules, and these findings suggest the significant potential of multi-zinc finger proteins as a tool for an artificial gene regulator.

Creating artificial transcription factors, which can activate or repress desired genes, is one of the most challenging and useful approaches for life science studies and clinical applications (*1, 2*). In order to target any gene, DNA binding proteins corresponding to each sequence are required. The C_2H_2-type zinc finger motif is one of the best frameworks to create new artificial DNA binding proteins (*1, 3*−*11*) for the following features (*12*): the zinc finger motif can (1) recognize continuous 3−4 bp[1] via key amino acid residues located on the recognition α-helix, (2) be tandemly repeated by covalent linkage, and (3) work as a monomer. By taking advantage of the first feature, artificial zinc finger proteins with the desired base recognition have been created by changing key amino acid residues on the recognition helix (*13*−*20*). The second feature has provided the artificial proteins with a long sequence binding property by connecting to one another (*21*−*30*). Finally, the monomeric binding mode offers a nonpalindromic binding sequence so that the target sequence could be flexibly selected. By fusing zinc finger motifs with a transcriptional activation or repression domain, artificial transcription factors targeting the desired genes are available (*31*−*33*). By fusing with a nuclease domain, specific sequence alterations can be created by homologous recombination (*34, 35*).

For application to a target in sequences as complex as the genome, the significantly strict specificity in DNA binding must be required (*21, 36*). A continuous 16 bp DNA sequence occurs in every 4^{16} or 4.3×10^9 bp, almost the same size as the human genome (3×10^9). Although a 6-finger protein that recognizes 18 bp can be sufficient to address a single site in the human genome, a longer targeting sequence is preferable, considering repetitive sequences that often occur in genomes and expecting much higher specificities in order to avoid any toxicity (*21, 36*). Our group has generated new zinc finger proteins by fusing 6, 9, and 15 motifs (multi-zinc finger protein) and shown that these proteins recognize approximately 18, 30, and as long as 50 bp, respectively (*23, 28*). Interestingly enough, we found that as the number of finger motifs increases, the time required for equilibrium with its target sequence is significantly longer: The equilibrium times are <0.5 h for the 3-finger, 48 h for the 6-finger, and 72 h for the 9- or 15-finger proteins. If this characteristic was maintained when applying *in vivo* for therapeutic use by fusing zinc finger motifs with an effector domain, it might be unfavorable in cases expecting

[†] This work was partially supported by a Grant-in-Aid for Scientific Research (20710165 for M.I.) from the Ministry of Education, Culture, Sports, Science and Technology, Japan. T.M. is a research fellow of the Japan Society for the Promotion of Science.

* To whom correspondence should be addressed. M.I.: phone, +81-774-38-3212; fax, +81-774-32-3038; e-mail, imiki@scl.kyoto-u.ac.jp. Y.S.: phone, +81-774-65-8649; fax, +81-774-65-8652; e-mail, ysugiura@dwc.doshisha.ac.jp.

[‡] Kyoto University.

[§] Japan Science and Technology Agency.

[||] Doshisha Women's University.

[1] Abbreviations: Tris, tris(hydroxymethyl)aminomethane; TN, Tris−NaCl; bp, base pair(s); AD, transcriptional activation domain; ER, estrogen receptor ligand binding domain; EMSA, electrophoretic mobility shift assay; PBS, phosphate-buffered saline.

10.1021/bi801124b CCC: $40.75
Published on Web 08/29/2008

rapid effects and avoiding the loss of function by its degradations.

We created 3- and 9-finger-type artificial transcription factors and extensively compared the kinetics of the transcriptional activation *in vivo* by introducing a ligand-inducing system. This report significantly shows that finger multimerization does not affect the kinetics of the transcriptional activity, suggesting the great potential of multi-zinc finger proteins.

MATERIALS AND METHODS

Chemicals. The T4 polynucleotide kinase and restriction enzymes were purchased from New England Biolabs, except for *Age*I obtained from Nippon Gene. The Taq DNA polymerase and synthesized oligonucleotides for cloning each gene and target sequence were acquired from Nippon Gene and Sigma-Genosys, respectively. The labeled [γ-^{32}P]ATP compound was supplied by Perkin-Elmer. The plasmid pBSKS+ ER^{TM} was kindly provided by Dr. Trevor D. Littlewood (*37*). All other chemicals were of commercial reagent grade.

Preparations of Zinc Finger Proteins and Target DNA Fragments. The DNA fragment coding ZF3, the 3-zinc finger region from murine transcription factor Zif268 (or Egr1) between the *Xma*I and *Age*I sites was generated by PCR using oligonucleotides as a template. For the 9-finger protein (ZF9), three units of the ZF3 coding DNA were fused sequentially with the *Xma*I and *Age*I sites so that each ligated sequence gives the canonical linker (-Thr-Gly-Glu-Arg-Pro-). The coding DNAs of ZF3 and ZF9 were then cloned into pEV-3b (*23*) and designated pEV-ZF3 and pEV-ZF9, respectively. Their sequences were confirmed by a GeneRapid DNA sequencer (Amersham Bioscience). The *Escherichia coli* strain BL21(DE3)pLysS was transformed with pEV-ZF3 and pEV-ZF9 and then incubated at 20 °C for 12 h under 0.1 mM IPTG and 0.1 mM $ZnCl_2$ condition to obtain the zinc finger proteins ZF3 and ZF9 as a soluble form, respectively. Overexpressed proteins were purified by cation-exchange chromatography using a High S column (Bio-Rad Laboratories) and Mono S column (Amersham Bioscience). The final purification was carried out using gel filtration chromatography with a Superdex 75 column (Amersham Bioscience). The fidelity of the purified ZF3 and ZF9 was confirmed by SDS−PAGE. The target DNA sequence of ZF3 was designated ZBS-I (5′-GCG-TGG-GCG-T-3′) (*12*). ZBS-III was designed as the repeat sequence of three units of ZBS-I for the ZF9 target DNA (5′-GCG-TGG-GCG-GCG-TGG-GCG-GCG-TGG-GCG-T-3′). The oligonucleotides containing either ZBS-I or ZBS-III and the complementary fragments were labeled with ^{32}P at the 5′-end by the T4 polynucleotide kinase before annealing. The annealed fragments were purified using a ProbeQuant G-50 column (GE Healthcare).

Electrophoretic Mobility Shift Assays (EMSA). EMSA were carried out under the following conditions. Each reaction mixture contained 10 mM Tris-HCl (pH 8.0), 50 mM NaCl, 1 mM dithiothreitol, 10 μM $ZnCl_2$, 0.05% Nonidet P-40, 25 ng/μL poly(dI-dC), 40 ng/μL bovine serum albumin, 5% glycerol, the ^{32}P-end-labeled target DNA fragment (25 pM, 250 cpm), and the serially diluted zinc finger protein (3-fold; 8.5 pM−500 nM). After incubation at 20 °C for 1, 3, 6, 24, 48, and 72 h, the samples were run on an 8% polyacrylamide gel with 89 mM Tris−borate buffer at 20 °C. The bands were visualized using STORM autoradiography (Amersham Bioscience) and analyzed by ImageQuant software (Molecular Dynamics). The equilibrium dissociation constants (K_d) of each protein−DNA fragment complex were evaluated by fitting the experimentally obtained values of θ_b (θ_b, the fraction of labeled DNA bound to the protein) to eq 1 using the Kaleida Graph program (Abelbeck software).

$$\theta_b = \frac{([P] + [D] + K_d) - \sqrt{([P] + [D] + K_d)^2 - 4[P][D]}}{2[D]} \quad (1)$$

Construction of Expression Vectors and Reporter Vectors for HeLa Cells. The pCMV-AD vector (Stratagene) contains the coding regions of the nuclear localization signal (NLS) from the SV40 large T-antigen and amino acids 364−550 of the murine NF-κB p65 (the transcriptional activation domain, AD) downstream of the CMV promoter, which is constitutively active in mammalian cell lines. To fuse a DNA binding domain at the N-terminus, unique 3′ cloning sites, containing *Eco*RI, in the pCMV-AD were replaced by a *myc* epitope tag sequence in frame with the AD, and new unique cloning sites were introduced between the CMV promoter and the coding region. The DNA fragment coding ZF3 and ZF9 acquired from pEV-ZF3 and pEV-ZF9, respectively, was inserted into pCMV-AD using *Sac*I and *Eco*RI to construct the pCMV-ZF3-NLS-AD and pCMV-ZF9-NLS-AD, respectively. For the ZF-ER-AD expression vectors, *Fse*I and *Spe*I were introduced with deletion of the NLS coding sequence. Two ERs (estrogen receptor ligand binding domain) flanked with *Fse*I and *Spe*I, and with *Nhe*I and *Asc*I, were constructed using the standard PCR technique with pBSKS+ ER^{TM} as the template (*37*) and sequentially cloned into pCMV-AD. Inserting ZF3 and ZF9 between the CMV promoter and the ER coding region produced pCMV-ZF3-ER-AD and pCMV-ZF9-ER-AD, respectively. The reporter vector used here was constructed by introducing the TATA box derived from herpes simplex virus thymidine kinase promoter into the pGL3-Basic vector (Promega) immediately upstream of the luc+ coding region and designated pGL3-TA. pGL3-TA/4xZBS-I and pGL3-TA/4xZBS-III each contain binding sites upstream of the TATA box. Their sequences were confirmed by a GeneRapid DNA sequencer.

Luciferase Reporter Assays. Fifty nanograms of the expression vector, 350 ng of the reporter vector, and 5 ng of the control vector (pRL-TK; Promega) were transiently cotransfected into HeLa cells using the Lipofectamin 2000 (Invitrogen). For all transfections, 6.5×10^4 HeLa cells per well were plated in 24-well dishes 2 days before and used at confluence. At 5 h after transfection, all cells were washed, and the medium was changed except for the cells harvested 6 h posttransfection. For the assays using the ZF-NLS-ADs, cell lysates were prepared at 6 and 48 h after transfection using passive lysis buffer (Promega). For the ZF-ER-ADs, the transcriptional activation potential was induced by the addition of 100 nM 4-hydroxytamoxifen (Sigma) at 24 h after transfection. Cell lysates were prepared 0, 1.5, 3, 6, 12, and 24 h postinduction using passive lysis buffer. The firefly and *renilla* luciferase activity was measured using the dual

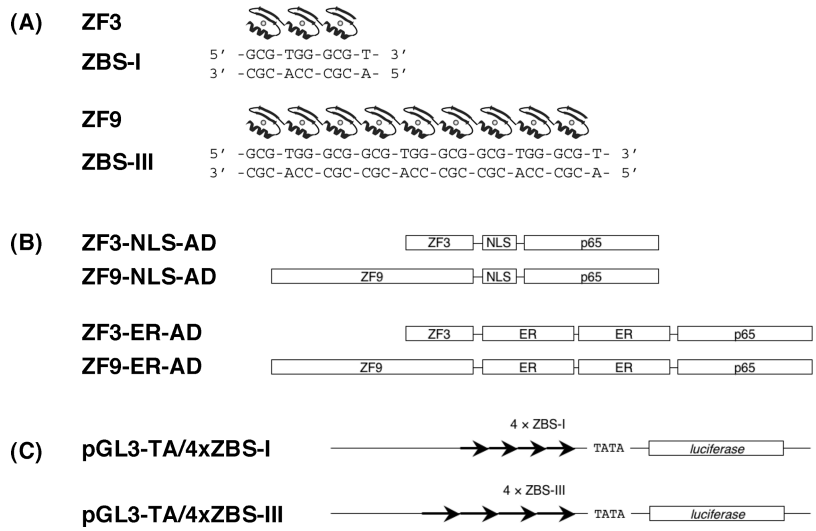

FIGURE 1: Schematic representation of ZF3, ZF9, and each target DNA sequence, ZBS-I and ZBS-III, respectively (A). Domain structure of artificial 3-finger- and 9-finger-type transcription factors, ZF-NLS-ADs; constitutively active transcription factors, ZF-ER-ADs; switchable transcription factors (B). Reporter constructs bearing 4 units of each target DNA sequence upstream of the TATA box (C).

luciferase reporter assay system (Promega). The luminescence (relative light units, RLU) was obtained by normalization to the transfection control and to the total amount of all proteins measured by the protein assay kit (Bio-Rad Laboratories).

Western Blot Analysis. Whole cell extracts were prepared at 24 h posttransfection in Laemmli buffer, and the total proteins were quantified using a protein assay kit (Bio-Rad Laboratories) according to the manufacturer's instruction. Whole cell extracts were separated on a polyacrylamide gel, SuperSep 5−20% (Wako), by electrophoresis with SDS−PAGE electrophoresis buffer (25 mM Tris-HCl, 192 mM glycine, and 0.1% SDS) and then transferred onto the Hybond-P polyvinylidene difluoride membrane (GE Healthcare). For each lane, the same amount of total protein was loaded on the gel for Western analysis. The membrane was then probed with anti-c-*Myc* antibody (9E10, Santa Cruz) or with anti-β-actin antibody (AC-15; Sigma) diluted in PBS containing 0.1% Tween 20 and 5% nonfat dry milk, followed by incubation with the second antibody (peroxidase-conjugated anti-mouse IgG; GE Healthcare). The antigen−antibody complexes were visualized with the ECL Plus Western blotting detection reagents (GE Healthcare) and captured with a LAS-3000 mini CCD imaging system (Fujifilm).

RESULTS

Prolonged Equilibrium Time by Finger Multimerization in Vitro. To evaluate the effect of finger multimerization on the DNA binding *in vitro*, the DNA binding characteristics of the 3-finger protein, ZF3, and the 9-finger protein, ZF9, were examined by electrophoretic mobility shift assays (EMSA) using ^{32}P-labeled DNA fragments with their target sequences, ZBS-I (10 bp) and ZBS-III (28 bp), respectively (Figure 1A). We first confirmed that ZF3 binds to ZBS-I and that ZF9 binds to ZBS-III (Figure 2). We then performed EMSA after various incubation times (1, 3, 6, 24, 48, and 72 h). The ratio of labeled DNA bound to the protein was plotted versus the protein concentration in Figure 3. The EMSA results revealed that ZF3 reached equilibrium with

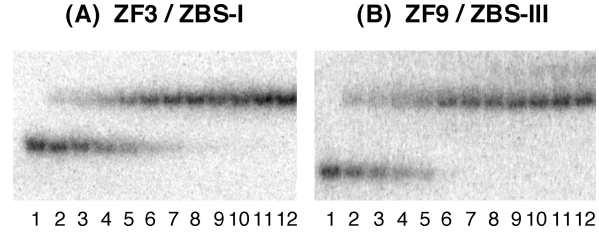

FIGURE 2: EMSA for binding of ZF3 to ZBS-I (A) and ZF9 to ZBS-III (B). Incubation at 20 °C for 48 h. Representative data are shown from three independent experiments.

ZBS-I within 6 h; on the other hand, ZF9 required as long as 72 h to be in equilibrium with ZBS-III. The apparent dissociation constants (K_d) were determined (Table 1) by fitting the plots at the equilibrium conditions to eq 1 in the Materials and Methods section. These results are consistent with our previous findings; i.e., an increase in the number of finger motifs can improve the DNA binding affinity but prolongs the equilibrium time (*23, 28*).

Design of Artificial Transcription Factors Based on Zinc Finger Motifs. In order to assess the effect of finger multimerization on the kinetics of the transcriptional activities *in vivo*, transcription factors that possess ZF3 and ZF9 as the DNA binding domain were designed (Figure 1B). The artificial transcription factors named ZF3-NLS-AD and ZF9-NLS-AD consist of ZF3 and ZF9 for their N-terminal, respectively, followed by the SV40 nuclear localization signal (NLS) and a transcriptional activation domain derived from NF-κB p65 (AD). For more precise analyses, the transcription factors termed ZF3-ER-AD and ZF9-ER-AD were engineered. The ZF-ER-ADs contain two units of estrogen receptor ligand binding domain (ER) instead of NLS, so that they work in a ligand-dependent manner. The linker used to connect the two ERs and the orientations of each domain were referenced to the report by Beerli et al. (*38*). In order to avoid constitutive activation, mutated ER (282−599, G525R), which is unable to bind estrogen and phenol red, yet retains normal affinity for the synthetic ligand, 4-hydroxytamoxifen (4-OHT), was used (*37*). pGL3-TA, pGL3-TA/4xZBS-I, and /4xZBS-III were used as reporter vectors (Figure 1C) for all transfections.

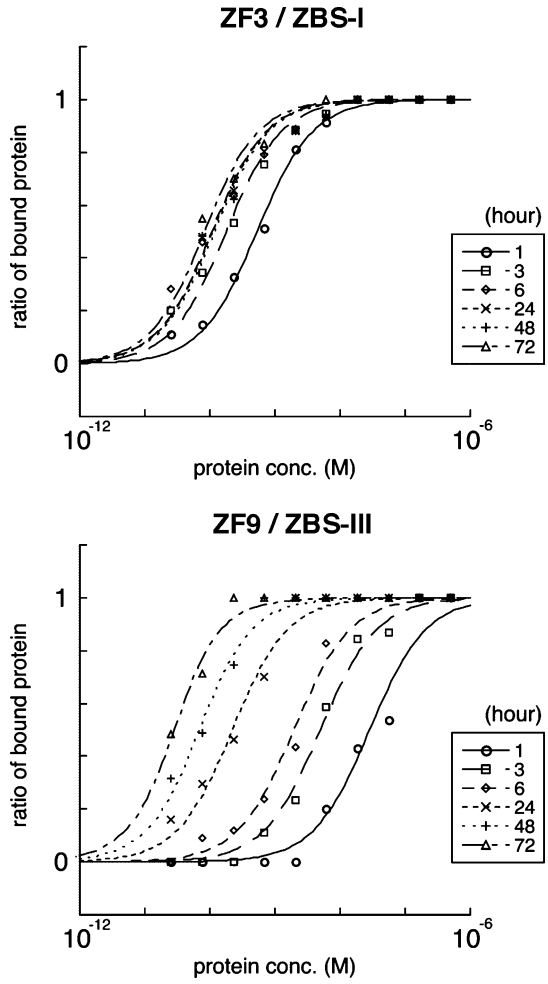

FIGURE 3: Prolonged equilibrium time of ZF9 with ZBS-III compared to ZF3 with ZBS-I. The EMSA results after 1, 3, 6, 24, 48, and 72 h of incubation were converted for the graph. The ratio of labeled DNA bound to the protein was plotted versus the protein concentration. The plots at each time point were temporarily fitted to eq 1 in the Materials and Methods, making it easier to interpret the results. Representative data were plotted from three independent experiments.

Table 1: Apparent Dissociation Constants (K_d) for ZF3 and ZF9 to ZBS-I and ZBS-III, Respectively

	ZF3/ZBS-I	ZF9/ZBS-III
K_d (pM)	129 ± 43.8	20.3 ± 6.8

The apparent dissociation constants were determined by titration using the gel mobility shift assay as described in the Materials and Methods section. The K_d for ZF3 was estimated from the EMSA data after 6 h incubation and ZF9 from 72 h. The values are averages ± SD of duplicate measurements.

Rapid Transcriptional Activation by Multifinger Type Transcription Factor in Vivo. As an expression vector, pCMV-ZF3-NLS-AD or pCMV-ZF9-NLS-AD was transiently cotransfected with each reporter vector, pGL3-TA/4xZBS-I or pGL3-TA/4xZBS-III, respectively, into HeLa cells. The relative luciferase activities after 6 and 48 h incubation are shown in Figure 4. After incubation for 48 h, both the 9-finger- and 3-finger-type transcription factors significantly activated the *luciferase* gene against the backgrounds that were transfected with pGL3-TA as a reporter vector. Likewise, intriguingly, the amount of luciferase was expressed greater by ZF9-NLS-AD than by ZF3-NLS-AD even at 6 h posttransfection.

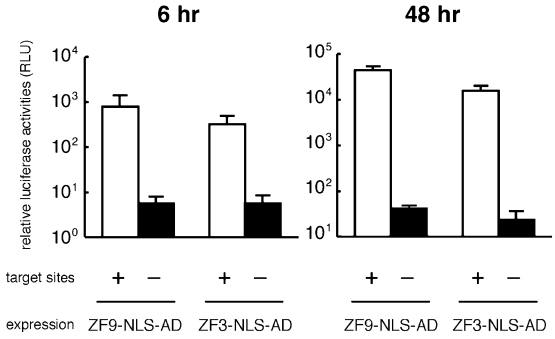

FIGURE 4: Significant activation of the reporter gene by ZF9-NLS-AD even 6 h after transfection. HeLa cells were cotransfected with expression vector encoding ZF9-NLS-AD or ZF3-NLS-AD and reporter vector bearing each target site (+) or lacking them (−) together with the control vector (pRL-TK). At 6 and 48 h after transfection, the firefly and *renilla* luciferase activities were measured. Each bar represents the mean value ± SD of three or more independent measurements.

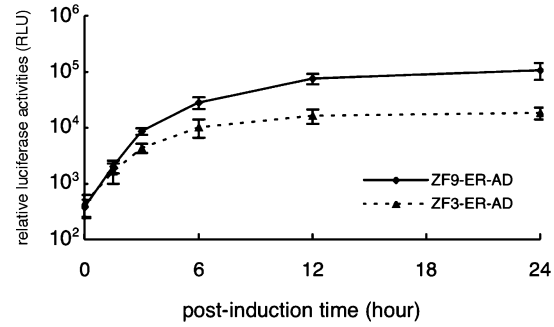

FIGURE 5: Prompt activation of the reporter gene by both ZF9-ER-AD and ZF3-ER-AD after ligand induction. HeLa cells were cotransfected with pCMV-ZF3-ER-AD or pCMV-ZF9-ER-AD and pGL3/4xZBS-I or pGL3/4xZBS-III, respectively, and the control vector (pRL-TK). At 24 h after transfection, 100 nM 4-OHT was added. Dual luciferase assays were performed at 0, 1.5, 3, 6, 12, and 24 h postinduction. Each dot represents the mean value ± SD of three or more independent measurements.

In order to more precisely explore these findings in detail, we adopted a switchable reporter assay system. We first confirmed the ligand dependency as follows. pCMV-ZF9-ER-AD, pCMV-ZF9-NLS-AD, pCMV-ZF3-ER-AD, or pCMV-ZF3-NLS-AD was cotransfected with each reporter vector and control vector (pRL-TK) into HeLa cells. At 24 h after transfection, the cells were treated with or without the ligand (4-OHT). Another 24 h later, cell lysates were prepared for the dual luciferase assays. The ZF-ER-ADs did not show a significant transcriptional activation property without ligand addition, although the ZF-NLS-ADs, as an experimental control, activated the reporter vectors in a ligand-independent manner (Supporting Information Figure 1). Figure 5 depicts the time-dependent luciferase activities promoted by ZF9- and ZF3-ER-AD. Supporting the results from assays using the ZF-NLS-ADs, ZF9-ER-AD activated the reporter gene as promptly as ZF3-ER-AD after the ligand addition, even though the equilibrium time of ZF9 to its target sequence *in vitro* is significantly longer than that of ZF3.

The expression levels of both ZF9-ER-AD and ZF3-ER-AD were examined by Western blot analysis (Figure 6) in order to determine whether this result, the prompt activation by ZF9-ER-AD, was caused by the stronger expression of ZF9-ER-AD than ZF3-ER-AD. The Western blot analysis revealed that the preinduction whole cell extracts contained

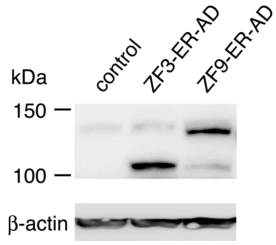

FIGURE 6: Expression levels of ZF9-ER-AD and ZF3-ER-AD. Whole cell extracts were prepared with 24 h posttransfection in Laemmli buffer and were analyzed by Western blot analysis using anti-c-*Myc* antibody. β-Actin was detected as an internal control. The representative data are shown from three independent experiments.

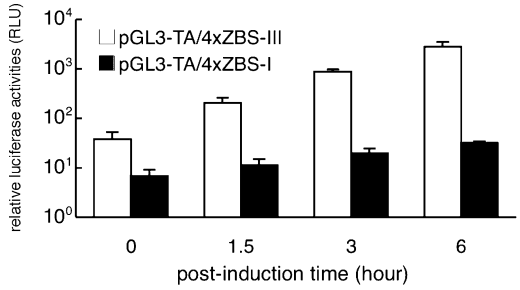

FIGURE 7: No significant activation of the reporter gene by the immature binding of ZF9-ER-AD. pCMV-ZF9-ER-AD were cotransfected with pGL3-TA/4xZBS-III or pGL3-TA/4xZBS-I, respectively, and the control vector (pRL-TK). Dual luciferase assays were performed using 0, 1.5, 3, and 6 h postinduction lysates. Each bar represents the mean value ± SD of three or more independent measurements.

almost the same amounts of ZF9-ER-AD and ZF3-ER-AD. However, a small amount of degradation products whose size was identical or very similar to ZF3-ER-AD was detected for ZF9-ER-AD.

The possibility of the activation by the immature binding of ZF9-ER-AD was then investigated. pCMV-ZF9-ER-AD was transiently transfected into HeLa cells together with the reporter vector bearing the incomplete binding sites, 4xZBS-I, instead of 4xZBS-III. Figure 7 shows that the transcription of the *luciferase* gene was not more significantly activated by ZF9-ER-AD from pGL3-TA/4xZBS-I when compared to pGL3-TA/4xZBS-III.

DISCUSSION

Multi-zinc finger proteins, which recognize long DNA sequences, are very useful as a DNA binding domain of artificial transcription factors (*31*−*33*), nucleases (*34, 35*), and so on in order to address single sites in complex sequences like genomes (*21, 36*). Our group has previously created multi-zinc fingers that recognize approximately 18, 30, and as long as 50 bp DNA sequences and also found that increasing the number of finger motifs improves the DNA binding selectivity and affinity but requires a longer time to reach equilibrium with its target DNA *in vitro* (*23, 28*). In this study, we demonstrated for the first time that finger multimerization does not affect the kinetics of the transcriptional activity *in vivo* when a zinc finger motif is used as a DNA binding domain for an artificial transcription factor.

For the finger multimerization, we have previously utilized the 3-zinc finger motif derived from the human transcription factor Sp1 and determined those DNA binding characteristics *in vitro* (*23, 25, 27*−*30*). Therefore, we have initially created Sp1-based artificial transcription factors and analyzed those transcriptional activities in HeLa cells so that we can take advantage of the previously acquired information. However, the reporter vector bearing the Sp1 target sequences was only slightly more activated when transfected with those transcription factors than without them. This might be due to the fact that most vertebrate cell types express some level of Sp1; thus assessing the characteristics of the Sp1-based artificial transcription factor in an ordinary vertebrate cell line is compromised. Therefore, we decided to adopt the 3-zinc finger motif from murine transcription factor, Zif268, which has already been used for many assays for mammalian cells (*18, 20*). The 9-finger protein, ZF9, was created by simply linking three units of the same 3-finger protein, ZF3, so that it was possible to directly assess the effect of multimerization by comparing the 9-finger protein to the 3-finger protein.

Since multi-zinc fingers based on Zif268 have not been exploited before, therefore we started out by assessing its DNA binding characteristics *in vitro*. Based on the results of the EMSA, ZF3 and ZF9 were ensured to interact with their target DNA sequence, ZBS-I and ZBS-III, respectively. We next performed EMSA for various incubation times, and the acquired ratio of labeled DNA bound to the protein was plotted versus the protein concentration. In order to interpret the time-dependent DNA binding manner, the plots at each time point were temporarily fitted to eq 1 as described in the Materials and Methods section, though the equation is exactly applicable only for equilibrium states. From the overlapping curve, it was revealed that ZF9 requires a much longer time (72 h) for reaching equilibrium with the target sequence than ZF3 (6 h). This difference may arise from the binding mode that ZF9, which recognizes the 28 bp DNA, has to wrap around an approximately 3-helical turn DNA duplex. It also may be due to lower affinity, but still significant affinity, interaction of component 3-fingers with the DNA in several different ways that do not allow full 9-finger binding. These binding complexes would then need to dissociate and rebind, perhaps multiple times, before the proper alignment was achieved that would allow higher, full 9-finger binding. The apparent dissociation constants (K_d) were determined from the fitting curve at each equilibrium state at 72 h for ZF9 and at 6 h for ZF3. As a result, the Zif268-based finger multimerization also improves the binding affinity to its target DNA. Those results are consistent with our previous findings; namely, an increase in the number of finger motifs can improve the DNA binding affinity but prolongs the equilibrium time (*23, 28*).

ZF9 needs a much longer time to reach equilibrium with the target DNA than ZF3; nevertheless, ZF9-NLS-AD, which simply fuses NLS and a transcriptional activation domain to ZF9, activated the reporter gene to a greater degree than ZF3-NLS-AD, not only at 48 h but also at 6 h posttransfection. Considering the time required for the expression of the ZF-NLS-ADs after transfection and for the expression of the luciferase after transcriptional activation, ZF9-NLS-AD has to start activating the reporter gene as rapidly as ZF3-NLS-AD. This result seems to conflict with that of *in vitro* experiments in which a multi-zinc finger needs a longer time for equilibrating with the target sequence.

Though the classical luciferase reporter assay system is simple and convenient, it has the following two drawbacks. One is that it takes time for the ZF-NLS-ADs to be expressed enough to produce a detectable amount of luciferase. This fact makes it difficult to analyze the transcriptional activities of the ZF-NLS-ADs in a short time posttransfection. The other is that the expressed ZF-NLS-ADs sequentially function as transcription factors and activate reporter vectors. Therefore, it is impossible to determine the time of onset and to precisely evaluate the time-dependent transcriptional activities.

To resolve these problems, the ZF-ER-ADs, whose function depends on ligand (4-OHT) addition, were designed by exchanging NLS with two units of the estrogen receptor ligand binding domains (*37, 38*). Introducing this switchable system made it possible to specify the onset time as the ligand addition time and to start each assay after a certain amount of preinduced ZF-ER-AD is accumulated. The time-dependent luciferase activities promoted by ZF-ER-AD were measured using lysates prepared by 0, 1.5, 3, 6, 12, and 24 h postinduction. The steep upstroke of the luciferase expression curve was observed not only for ZF3-ER-AD but also for ZF9-ER-AD. This result further supports our assumption that ZF9-NLS-AD activates the reporter gene as rapidly as ZF3-NLS-AD. In addition, when the expression level of the luciferase reached a plateau, the expression level by ZF9-ER-AD was approximately 6-fold higher than that by ZF3-ER-AD. This result agrees with the previous study that the functional activity of zinc finger-based artificial transcription factors *in vivo* is positively correlated with its binding affinity *in vitro* (*39*).

However, the present rapid activation of ZF9-ER-AD may arise from the result of the stronger expression of ZF9-ER-AD than ZF3-ER-AD. It may also arise from the result of the immature binding of ZF9-ER-AD. Since the ZF9 is constituted of three units of the ZF3, we must consider that 3 fingers worth of binding might be sufficient for the transcriptional activity. Therefore, we performed a Western blot analysis to ascertain the expression levels of ZF9-ER-AD and ZF-3-ER-AD and also a reporter vector assay using incomplete binding sites to examine the effects of the immature binding of ZF9-ER-AD. The Western blot analysis suggested almost the same expression levels of ZF9-ER-AD (126.8 kDa) and ZF3-ER-AD (106.4 kDa). The possibility that a higher expression level of ZF9-ER-AD than by ZF3-ER-AD causes its prompt activation can be denied, but the Western blot exhibited a degradation product whose size was identical or very similar to ZF3-ER-AD for ZF9-ER-AD. We then performed a luciferase reporter assay for ZF9-ER-AD with the reporter vector possessing 4xZBS-I as the binding sites. Consequently, ZF9-ER-AD showed a slight, but no significant activation for pGL3-TA/4xZBS-I. This result proved that the immature binding of ZF9-ER-AD had little or no effect on the activation and is consistent with a previous work (*40*). In addition, considering that the degree of activation for pGL3-TA/4xZBS-I was much lower than that for /4xZBS-III, no significant contribution could be expected by the degradation product from ZF9-ER-AD to the prompt activation, even though the degradation product was postulated as ZF3-ER-AD.

Our results indicate that the drawback of finger multimerization, namely, prolongation of the equilibrium time depending on the number of finger motifs, can be surmounted in terms of its use for transcription factors *in vivo*. Presumably, this is due to the intracellular environment, for example, a molecular crowding effect (*41*−*43*), existence of proteins with chaperone-like activities that facilitate the interaction between zinc finger motif and its target DNA (*44, 45*), and/or due to the large amount of artificial transcription factors compared to the reporter vector introduced into the cell. There is much interest in creating therapeutic molecules. Although further studies are necessary to uncover the behaviors of the artificial transcription factors based on a zinc finger motif *in vivo*, our findings suggest the significant potential of multi-zinc finger proteins as a tool for an artificial gene regulator.

ACKNOWLEDGMENT

We thank Dr. Trevor D. Littlewood for kindly providing the plasmid pBSKS+ ER™.

SUPPORTING INFORMATION AVAILABLE

Figure S1 showing the ligand dependency of ZF-ER-ADs on the luciferase assay. This material is available free of charge via the Internet at http://pubs.acs.org.

REFERENCES

1. Blancafort, P., Segal, D. J., and Barbas, C. F., III (2004) Designing transcription factor architectures for drug discovery. *Mol. Pharmacol. 66*, 1361–1371.
2. Koh, J. T., and Zheng, J. (2007) The new biomimetic chemistry: artificial transcription factors. *ACS Chem. Biol. 2*, 599–601.
3. Imanishi, M., Hori, Y., Nagaoka, M., and Sugiura, Y. (2001) Design of novel zinc finger proteins: towards artificial control of specific gene expression. *Eur. J. Pharm. Sci. 13*, 91–97.
4. Pabo, C. O., Peisach, E., and Grant, R. A. (2001) Design and selection of novel Cys2His2 zinc finger proteins. *Annu. Rev. Biochem. 70*, 313–340.
5. Beerli, R. R., and Barbas, C. F., III (2002) Engineering polydactyl zinc-finger transcription factors. *Nat. Biotechnol. 20*, 135–141.
6. Jamieson, A. C., Miller, J. C., and Pabo, C. O. (2003) Drug discovery with engineered zinc-finger proteins. *Nat. Rev. Drug Discovery 2*, 361–367.
7. Jantz, D., Amann, B. T., Jr., and Berg, J. M. (2004) The design of functional DNA-binding proteins based on zinc finger domains. *Chem. Rev. 104*, 789–799.
8. Papworth, M., Kolasinska, P., and Minczuk, M. (2006) Designer zinc-finger proteins and their applications. *Gene 366*, 27–38.
9. Wu, J., Kandavelou, K., and Chandrasegaran, S. (2007) Custom-designed zinc finger nucleases: what is next? *Cell. Mol. Life Sci. 64*, 2933–2944.
10. Negi, S., Imanishi, M., Matsumoto, M., and Sugiura, Y. (2008) New redesigned zinc-finger proteins: design strategy and its application. *Chem. Eur. J. 14*, 3236–3249.
11. Blancafort, P., and Beltran, A. S. (2008) Rational design, selection and specificity of artificial transcription factors (ATFs): the influence of chromatin in target gene regulation. *Comb. Chem. High Throughput Screen. 11*, 146–158.
12. Pavletich, N. P., and Pabo, C. O. (1991) Zinc finger-DNA recognition: crystal structure of a Zif268-DNA complex at 2.1 Å. *Science 252*, 809–817.
13. Rebar, E. J., and Pabo, C. O. (1994) Zinc finger phage: affinity selection of fingers with new DNA-binding specificities. *Science 263*, 671–673.
14. Jamieson, A. C., Wang, H., and Kim, S. H. (1996) A zinc finger directory for high-affinity DNA recognition. *Proc. Natl. Acad. Sci. U.S.A. 93*, 12834–12839.
15. Choo, Y., Castellanos, A., García-Hernndez, B., Snchez-García, I., and Klug, A. (1997) Promoter-specific activation of gene expression directed by bacteriophage-selected zinc fingers. *J. Mol. Biol. 273*, 525–532.
16. Greisman, H. A., and Pabo, C. O. (1997) A general strategy for selecting high-affinity zinc finger proteins for diverse DNA target sites. *Science 275*, 657–661.

17. Segal, D. J., Dreier, B., Beerli, R. R., and Barbas, C. F., III (1999) Toward controlling gene expression at will: Selection and design of zinc finger domains recognizing each of the 5′-GNN-3′ DNA target sequences. *Proc. Natl. Acad. Sci. U.S.A. 96*, 2758–2763.
18. Dreier, B., Beerli, R. R., Segal, D. J., Flippin, J. D., and Barbas, C. F., III (2001) Development of zinc finger domains for recognition of the 5′-ANN-3′ family of DNA sequences and their use in the construction of artificial transcription factors. *J. Biol. Chem. 276*, 29466–29478.
19. Sera, T., and Uranga, C. (2002) Rational design of artificial zinc-finger proteins using a nondegenerate recognition code table. *Biochemistry 41*, 7074–7081.
20. Dreier, B., Fuller, R. P., Segal, D. J., Lund, C. V., Blancafort, P., Huber, A., Koksch, B., and Barbas, C. F., III (2005) Development of zinc finger domains for recognition of the 5′-CNN-3′ family DNA sequences and their use in the construction of artificial transcription factors. *J. Biol. Chem. 280*, 35588–35597.
21. Liu, Q., Segal, D. J., Ghiara, J. B., and Barbas, C. F., III (1997) Design of polydactyl zinc-finger proteins for unique addressing within complex genomes. *Proc. Natl. Acad. Sci. U.S.A. 94*, 5525–5530.
22. Beerli, R. R., Segal, D. J., Dreier, B., and Barbas, C. F., III (1998) Toward controlling gene expression at will: specific regulation of the erbB-2/HER-2 promoter by using polydactyl zinc finger proteins constructed from modular building blocks. *Proc. Natl. Acad. Sci. U.S.A. 95*, 14628–14633.
23. Kamiuchi, T., Abe, E., Imanishi, M., Kaji, T., Nagaoka, M., and Sugiura, Y. (1998) Artificial nine zinc-finger peptide with 30 base pair binding sites. *Biochemistry 37*, 13827–13834.
24. Kim, J. S., and Pabo, C. O. (1998) Getting a handhold on DNA: design of poly-zinc finger proteins with femtomolar dissociation constants. *Proc. Natl. Acad. Sci. U.S.A. 95*, 2812–2817.
25. Imanishi, M., Hori, Y., Nagaoka, M., and Sugiura, Y. (2000) DNA-bending finger: artificial design of 6-zinc finger peptides with polyglycine linker and induction of DNA bending. *Biochemistry 39*, 4383–4390.
26. Moore, M., Choo, Y., and Klug, A. (2001) Design of polyzinc finger peptides with structured linkers. *Proc. Natl. Acad. Sci. U.S.A. 98*, 1432–1436.
27. Imanishi, M., and Sugiura, Y. (2002) Artificial DNA-bending six-zinc finger peptides with different charged linkers: distinct kinetic properties of DNA bindings. *Biochemistry 41*, 1328–1334.
28. Hirata, T., Nomura, W., Imanishi, M., and Sugiura, Y. (2005) Effects of linking 15-zinc finger domains on DNA binding specificity and multiple DNA binding modes. *Bioorg. Med. Chem. Lett. 15*, 2197–2201.
29. Imanishi, M., Yan, W., Morisaki, T., and Sugiura, Y. (2005) An artificial six-zinc finger peptide with polyarginine linker: selective binding to the discontinuous DNA sequences. *Biochem. Biophys. Res. Commun. 333*, 167–173.
30. Yan, W., Imanishi, M., Futaki, S., and Sugiura, Y. (2007) α-Helical linker of an artificial 6-zinc finger peptide contributes to selective DNA binding to a discontinuous recognition sequence. *Biochemistry 46*, 8517–8524.
31. Dent, C. L., Lau, G., Drake, E. A., Yoon, A., Case, C. C., and Gregory, P. D. (2007) Regulation of endogenous gene expression using small molecule-controlled engineered zinc-finger protein transcription factors. *Gene Ther. 14*, 1362–1369.
32. Shieh, J. C., Cheng, Y. C., Su, M. C., Moore, M., Choo, Y., and Klug, A. (2007) Tailor-made zinc-finger transcription factors activate FLO11 gene expression with phenotypic consequences in the yeast Saccharomyces cerevisiae. *PLoS ONE 2*, e746.
33. Blancafort, P., Tschan, M. P., Bergquist, S., Guthy, D., Brachat, A., Sheeter, D. A., Torbett, B. E., Erdmann, D., and Barbas, C. F., III (2008) Modulation of drug resistance by artificial transcription factors. *Mol. Cancer Ther. 7*, 688–697.
34. Urnov, F. D., Miller, J. C., Lee, Y. L., Beausejour, C. M., Rock, J. M., Augustus, S., Jamieson, A. C., Porteus, M. H., Gregory, P. D., and Holmes, M. C. (2005) Highly efficient endogenous human gene correction using designed zinc-finger nucleases. *Nature 435*, 646–651.
35. Mani, M., Kandavelou, K., Dy, F. J., Durai, S., and Chandrasegaran, S. (2005) Design, engineering, and characterization of zinc finger nucleases. *Biochem. Biophys. Res. Commun. 335*, 447–457.
36. Cornu, T. I., Thibodeau-Beganny, S., Guhl, E., Alwin, S., Eichtinger, M., Joung, J. K., and Cathomen, T. (2008) DNA-binding specificity is a major determinant of the activity and toxicity of zinc-finger nucleases. *Mol. Ther. 16*, 352–358.
37. Littlewood, T. D., Hancock, D. C., Danielian, P. S., Parker, M. G., and Evan, G. I. (1995) A modified oestrogen receptor ligand-binding domain as an improved switch for the regulation of heterologous proteins. *Nucleic Acids Res. 23*, 1686–1690.
38. Beerli, R. R., Schopfer, U., Dreier, B., and Barbas, C. F., III (2000) Chemically regulated zinc finger transcription factors. *J. Biol. Chem. 275*, 32617–32627.
39. Kang, J. S. (2007) Correlation between functional and binding activities of designer zinc-finger proteins. *Biochem. J. 403*, 177–182.
40. Yant, S. R., Huang, Y., Akache, B., and Kay, M. A. (2007) Site-directed transposon integration in human cells. *Nucleic Acids Res. 35*, e50.
41. Ellis, R. J. (2001) Macromolecular crowding: an important but neglected aspect of the intracellular environment. *Curr. Opin. Struct. Biol. 11*, 114–119.
42. Sasaki, Y., Miyoshi, D., and Sugimoto, N. (2006) Effect of molecular crowding on DNA polymerase activity. *Biotechnol. J. 1*, 440–446.
43. Sasaki, Y., Miyoshi, D., and Sugimoto, N. (2007) Regulation of DNA nucleases by molecular crowding. *Nucleic Acids Res. 35*, 4086–4093.
44. Cruceanu, M., Gorelick, R. J., Musier-Forsyth, K., Rouzina, I., and Williams, M. C. (2006) Rapid kinetics of protein-nucleic acid interaction is a major component of HIV-1 nucleocapsid protein's nucleic acid chaperone function. *J. Mol. Biol. 363*, 867–877.
45. Roemer, S. C., Adelman, J., Churchill, M. E., and Edwards, D. P. (2008) Mechanism of high-mobility group protein B enhancement of progesterone receptor sequence-specific DNA binding. *Nucleic Acids Res. 36*, 3655–3666.

BI801124B